Theoret. Appl. Mech., Vol.33, No.4, pp. 281–309, Belgrade 2006

Hall effect on MHD mixed convection flow of a viscoelastic fluid past an infinite vertical porous plate with mass transfer and radiation

R.C.Chaudhary * **Preeti Jain** †

Abstract

An unsteady hydro-magnetic flow of a viscoelastic fluid from a radiative vertical porous plate has been studied with mass transfer, taking the effect of Hall currents into account. The resulting problem has been solved analytically and the closed form solutions are obtained for velocity, temperature and concentration distributions as well as for the shearing stress, rate of heat and mass transfer at the wall. The influence of the various parameters like Hall parameter, magnetic parameter, visco-elastic parameter, frequency parameter etc. on the flow field is examined with the help of figures and tables.

Keywords: hall effect, viscoelastic fluid, radiative transfer, mass transfer, mixed-convection.

1 Introduction

Many transport processes can be found in various ways in both nature and technology, in which the combined heat and mass transfer occur due

*Department of Mathematics, University of Rajasthan, Jaipur-302004, India, e-mail: rcchaudhary@rediffmail.com

†Department of Mathematics, University of Rajasthan, Jaipur-302004, India, e-mail: jainpreeti28@rediffmail.com

to buoyancy forces caused by thermal diffusion (temperature differences) and mass diffusion (concentration differences). Some of the convective heat and mass transfer processes with phase change include the evaporation of liquid at the interface between a gas and liquid or the sublimation at a solid-gas interface. They can be described using the methods of convective heat and mass transfer. The process of mass transfer affects all separation processes in chemical engineering such as the drying of solid materials, distillation, extraction and absorption. They also play a role in the production of materials of desired properties. Mass transfer often decisively determines chemical reactions, including combustion processes. Boiling and condensation are characteristic for many separation processes in chemical engineering. As examples of these types of processes, the evaporation, rectification and absorption of a fluid should all be mentioned (Baehr et al. [1]).

Natural convection induced by the simultaneous action of buoyancy forces resulting from thermal and mass diffusion is of considerable interest in many industrial applications such as geophysics, oceanography, drying processes and solidification of binary alloy. Soundalgekar [2], Soundalgekar et al. [3], Perdikis et al. [4], and Lin et al. [5] are some of the researchers who have studied the heat and mass transfer from a vertical plate. The effect of the magnetic field on free convection flows is important in liquid metals, electrolytes and ionized gases. The thermal physics of MHD problems with mass transfer is of interest in power engineering and metallurgy. Many cross galvano and thermo-magnetic effects occur in the boundary zone between hydraulics and thermal physics and they are relevant in the study of semiconductor materials. The mechanism of conduction in ionized gases in the presence of a strong magnetic field is different from that in a metallic substance. The electric current in ionized gases is generally carried by electrons which undergo successive collisions with other charged or neutral particles. In the ionized gases the current is not proportional to the applied potential except when the electric field is very weak. However, in the presence of strong electric field, the electrical conductivity is affected by the magnetic field. Consequently, the conductivity parallel to the electric field is reduced. Hence the current is reduced in the direction normal to both electric and magnetic fields. This phenomenon is known as the Hall Effect. The effect of magnetic field (without Hall effect) on the unsteady free convection flow over an infinite vertical porous plate has been considered by Georgantopoulos et al. [6] and Helmy [7]. The effect of Hall current on unsteady MHD free convection flow along a vertical porous plate has been studied by Katagiri [8], Hossain [9], Hossain et al. [10], Pop et al. [11] and Acharya et al. [12]. The unsteady free convection flow over an infinite vertical porous plate due to the combined effects of thermal and mass diffusion along with

Hall currents have been considered by Hossain et al. [13], Aboeldahab et al. [14] and Takhar et al. [15].

All the above investigations are restricted to MHD flow and heat transfer problems. However, when the free convective flows occur at high temperatures, radiation effects on the flow become significant. Many processes in engineering areas occur at high temperatures and knowledge of radiative heat transfer becomes very important for the design of the pertinent equipment. Nuclear power plants, gas turbines and the various propulsion devices for aircraft, missiles and space vehicles are examples of such engineering areas. The inclusion of radiation effects in the energy equation leads to a highly non-linear partial differential equation. Soundalgekar and Takhar[16] have studied radiation effects on the free convection flow of a gas past a semi-infinite plate using Cogley-Vincentine-Giles equilibrium model. Takhar [17] investigated the effects of radiation on the MHD free convection flow past a semi-infinite vertical plate. Radiation effect on mixed convection along an isothermal vertical plate was studied by Hossain and Takhar [18] using Rosseland approximation while Abo-elahab [19] discussed this problem using Cogley-Vincentine-Giles equilibrium model. Recently, Muthucumaraswamy et al. [20] discussed the heat and mass transfer effects on moving vertical plate in the presence of thermal radiation. Kinyanjui et al. [21] analysed heat and mass transfer of heat generating fluid past a vertical porous plate with Hall current and radiation absorption.

All the studies cited above are restricted to the flow of Newtonian fluids. However in reality, most of the liquids used in industrial applications, particularly in polymer processing applications, molten plastics, food stuffs or slurries, display non-Newtonian behaviour. Rajagopal [22] investigated the heat transfer in the forced convection flow of a visco-elastic fluid of Walters's model. Chowdhury et al. [23] studied the MHD free convection flow of visco-elastic fluid past a vertical porous plate. Bestman [24] included the radiation effect on free convection heat transfer flow of non-Newtonian fluid.

In all these studies, the combined effects of mass and radiative heat transfer of visco-elastic fluid in addition to Hall currents have not been considered simultaneously. We now propose to study the effect of radiation heat absorption and mass transfer on the flow of visco-elastic fluid past an infinite vertical porous plate taking Hall Effect into the account.

2 Mathematical Analysis

We consider the unsteady free convection flow of a viscous, incompressible, electrically conducting fluid on an infinite vertical permeable plate located at the plane $y^* = 0$. The x^*-axis is chosen along the plate in the upward direction and y^*-axis is taken perpendicular to the plate. Hall currents give rise to the Lorentz force in z^*-direction which induces a cross flow in that direction. Consequently, the flow field becomes three dimensional. The z^*-axis is assumed to be normal to the $x^* - y^*$ plane. The fluid is assumed to be gray, emitting and absorbing heat but not scattering and subjected to a transversely applied uniform magnetic field of strength B_0. Since the plate is infinite in extent all the physical quantities are function of y^* and t^* only. At time $t^* > 0$, the plate is kept at the oscillating temperature and concentration.

The constitutive equations for the rheological equation of state for visco-elastic fluid (Walters's liquid B') are:

$$p_{ik} = -pg_{ik} + p^*_{ik} \tag{1}$$

$$p^{*ik} = 2\int_{-\infty}^{t} \psi(t - t^*) e^{(1)}_{ik}(t^*) dt^* \tag{2}$$

in which

$$\psi(t - t^*) = \int_0^\infty \frac{N(\tau)}{\tau} e^{(-(t-t^*)/\tau)} d\tau \tag{3}$$

$N(\tau)$ is the distribution function of relaxation times τ. In the above equations p_{ik} is the stress tensor, p an arbitrary isotropic pressure, g_{ik} is the metric tensor of a fixed coordinate system x^i and e_{ik} (1) is the rate of strain tensor. It was shown by Walters [25] that equation (2) can be put in the following generalized form which is valid for all types of motion and stress

$$p^{*\,ik}(x,t) = 2\int_{-\infty}^{t} \psi(t-t^*) \frac{\partial x^i}{\partial x^{*m}} \frac{\partial x^k}{\partial x^{*r}} e^{(1)\,mr}\,(x^* t^*)\,dt^* \tag{4}$$

where $x^{*i} = x^{*i}(x,t,t^*)$ is the position at time t^* of the element which is instantaneously at the position x^i at time t. The fluid with equation of state (1) and (4) has been designated as liquid B'. In the case of liquids with short memories, i.e. short relaxation times, the above equation of state can be written in the following simplified form

$$p^{*\,ik}(x,t) = 2\eta_0\, e^{(1)\,ik} - 2k_0 \frac{\partial e^{(1)\,ik}}{\partial t} \tag{5}$$

where $\eta_0 = \int_0^\infty N(\tau)\,d\tau$ is limiting viscosity at small rates of shear. $k_0 = \int_0^\infty \tau\, N(\tau) d\tau$ and $\frac{\partial}{\partial t}$ denotes the convected time derivative.

Hence the equations governing the flow of fluid together with Maxwell's electromagnetic equations are expressed as:-

Continuity equation

$$\nabla.\vec{V} = 0 \tag{6}$$

Momentum equation

$$\frac{\partial \vec{V}}{\partial t^*} + (\vec{V}\,.\nabla)\,\vec{V} = -\frac{1}{\rho}\nabla P + \nu\,\nabla^2\vec{V} + \nabla.\,p_{ij} + \\ g\beta\,(T^* - T^*_\infty) + g\beta_c(C^* - C^*_\infty) + \frac{1}{\rho}\,(\vec{J}\,x\vec{B}) \tag{7}$$

Energy equation

$$\frac{\partial T^*}{\partial t^*} + (\vec{V}.\nabla)\,T^* = \frac{K}{\rho\, c_p}\nabla^2\, T^* - \frac{1}{\rho\, c_p}\nabla\, q_r \tag{8}$$

Species Concentration equation

$$\frac{\partial C^*}{\partial t^*} + (\vec{V}.\nabla)\,C^* = D\nabla^2\, C^* \tag{9}$$

Generalized Ohm's law

$$\vec{J} = \sigma(\vec{E} + \vec{V}\,x\vec{B}) - \frac{\sigma}{en_e}(\vec{J}\,x\vec{B} - \nabla P_e) \tag{10}$$

Maxwell's equations

$$\nabla\, x\vec{\mathrm{H}} = \vec{J}\,,\ \nabla\, x\vec{E} = 0\,,\ \nabla\,.\,\vec{B} = 0 \tag{11}$$

Here $\vec{V}(u^*, v^*, w^*)$ is the velocity vector, u^*, v^*, w^* are the velocity components along x^*, y^*, z^* directions, $\vec{B}(0, B_0, 0)$ is the magnetic induction, $\vec{E}(E_{x*}, E_{y*}, E_{z*})$ is the electric field vector, E_{x*}, E_{y*}, E_{z*} are the components of electric field along x^*, y^*, z^* directions, $\vec{H}$ is the magnetic field strength vector, $\vec{J}(J_{x*}, J_{y*}, J_{z*})$ is the current density vector, J_{x*}, J_{y*}, J_{z*} are the components of current density along x^*, y^*, z^* directions , P is the pressure of fluid, P_e is the electron density, p_{ij} is the stress tensor, q_r is the radiative heat flux, e is the electron charge, n_e is electron number density, T^*_∞ is the temperature of the fluid far away from the plate, C^*_∞ is the species concentration far away from the plate, K is thermal conductivity, c_p is specific heat at constant pressure, ρ is the density, σ is the electrical conductivity, β is the volumetric coefficient of thermal expansion, β_c is volumetric coefficient of expansion with concentration, g is acceleration due to gravity, D is the chemical molecular diffusivity, ν is the kinematic viscosity.

In addition, the analysis is based on the following assumptions:

1. The equation of continuity (6) on integration gives

$$v^* = \ constant = -\,v_0,\ v_0 > 0 \tag{12}$$

   where v_0 is the constant normal velocity of suction at the plate.

2. The divergence equation of magnetic field $\nabla.\,\vec{B} = 0$ gives $B_{y*} = constant = B_0$

   By assuming a very small magnetic Reynolds number ($Re_m = \mu_m \sigma \vec{V} L << 1$) the induced magnetic field is neglected in comparison to the applied magnetic field so that $B_{y*} = B_{z*} = 0$ hence $\vec{B} = (0, B_0, 0)$.

   Here L is the characteristic length and μ_m is the magnetic permeability.

3. Since no polarization voltage is imposed on the flow field, the electric field vector $\vec{E} = 0$, this then corresponds to the case when no energy is added or extracted from the fluid by the electric field.

4. The equation of conservation of charge $\nabla.\vec{J} = 0$ gives, $Jy^* = constant$. Since the plate is not conducting $J_{y*} = 0$ at the plate, and, hence zero everywhere.

5. Considering the magnetic field strength to be very large the generalized Ohm's law including Hall current in the absence of electric field takes the following form:

$$\vec{J} + \frac{\omega_e \tau_e}{B_0} (\vec{J} x \vec{B}) = \sigma \left(\vec{V} x \vec{B} + \frac{\nabla P_e}{e n_e} \right) \tag{13}$$

where ω_e is the electron frequency and τ_e is the electron collision time. For weakly ionized gases the thermoelectric pressure and ion slip are considered negligible.

Equation (8) reduces to

$$J_{x*} = \frac{\sigma B_0}{1 + m^2} (mu^* - w^*) \tag{14}$$

$$J_{z*} = \frac{\sigma B_0}{1 + m^2} (u^* + mw^*) \tag{15}$$

where $m = \omega_e \tau_e$ is the Hall parameter. Thus the governing equations of flow under the usual Boussinesq approximation now become:

Momentum equation

$$\frac{\partial u^*}{\partial t^*} - v_0 \frac{\partial u^*}{\partial y^*} = \nu \frac{\partial^2 u^*}{\partial y^{*2}} - k_0 \frac{\partial^3 u^*}{\partial y^{*2} \partial t^*} - \frac{\sigma B_0^2 (u^* + mw^*)}{\rho(1 + m^2)} +$$

$$g\beta (T^* - T^*_\infty) + g\beta_c (C^* - C^*_\infty) \tag{16}$$

$$\frac{\partial w^*}{\partial t^*} - v_0 \frac{\partial w^*}{\partial y^*} = \nu \frac{\partial^2 w^*}{\partial y^{*2}} - k_0 \frac{\partial^3 w^*}{\partial y^{*2} \partial t^*} + \frac{\sigma B_0^2 (mu^* - w^*)}{\rho (1 + m^2)} \tag{17}$$

Energy equation

$$\frac{\partial (T^* - T^*_\infty)}{\partial t^*} - v_0 \frac{\partial (T^* - T^*_\infty)}{\partial y^*} = \frac{K}{\rho c_p} \frac{\partial^2 (T^* - T^*_\infty)}{\partial y^{*2}} - \frac{1}{\rho c_p} \frac{\partial q_r}{\partial y^*} \tag{18}$$

Species concentration equation

$$\frac{\partial (C^* - C^*_\infty)}{\partial t^*} - v_0 \frac{\partial (C^* - C^*_\infty)}{\partial y^*} = D \frac{\partial^2 (C^* - C^*_\infty)}{\partial y^{*2}} \tag{19}$$

By using the Cogley et al. [26] relation, the radiative heat flux (q_r) for the optically thin limit non-gray gas near equilibrium is given by:

$$\frac{\partial q_r}{\partial y^*} = 4I(T^* - T^*_\infty) \quad \text{where} \quad I = \int_0^\infty K_{\lambda w} \left(\frac{\partial e_{b\lambda}}{\partial T^*} \right)_w d\lambda \tag{20}$$

Here $K_{\lambda w}$ is the mean absorption coefficient, $e_{b\lambda}$ is Plank's function and T^* is the temperature.

In equation (18) the viscous dissipation and Ohmic dissipation are neglected and in equation (19) the term due to chemical reaction is assumed to be absent. Using $T^*(y^*, t^*) - T^*_\infty = \theta^*(y^*, t^*)$ in equation (18) and $C^*(y^*, t^*) - C^*_\infty = \bar{C}(y^*, t^*)$ in equation (19) subjecting to the initial and boundary conditions:

$$\left.\begin{array}{l}
t^* \le 0 : \left.\begin{array}{l} u^*(y^*, t^*) = w^*(y^*, t^*) = 0 \\ \theta^*(y^*, t^*) = 0, \ \bar{C}(y^*, t^*) = 0 \end{array}\right\} \quad \text{for all} \quad y^* \\[2ex]
t^* > 0 : u^*(0, t^*) = 0, \quad w^*(0, t^*) = 0, \quad \theta^*(0, t^*) = a e^{i\omega^* t^*} \\
\qquad\quad \bar{C}(0, t^*) = b e^{i\omega^* t^*} \\[2ex]
\qquad\quad : u^*(\infty, t^*) = w^*(\infty, t^*) = \theta^*(\infty, t^*) = \bar{C}(\infty, t^*) = 0
\end{array}\right\} \tag{21}$$

where ω^* is frequency of oscillations, a and b are taken as temperature and concentration difference respectively and subscript w and ∞ denotes the physical quantities at the plate and in the free stream respectively and using the following non-dimensional parameters:

$$\eta = \frac{v_0\, y^*}{\nu}\ ,\ t = \frac{v_0^2\, t^*}{4\nu}\ ,\ \Omega = \frac{4\nu\, \omega^*}{v_0^2}\ ,$$

$$u = \frac{u^*}{v_0}\ ,\ w = \frac{w^*}{v_0}\ ,\ \theta = \frac{\theta^*}{a}\ ,\ C = \frac{\bar{C}}{b}\ ,$$

$$Gr = \frac{4g\beta\nu\, a}{v_0^3}\ ,\ Gc = \frac{4g\beta_c\, \nu\, b}{v_0^3}\ ,\ M = \frac{4\sigma\, B_0^2\, \nu}{\rho\, v_0^2}\ ,\ Pr = \frac{\mu\, c_p}{K}\ ,$$

$$Sc = \frac{\nu}{D}\ ,\ F = \frac{16\, \nu\, I}{v_0^2\, \rho\, c_p}\ ,\ k = \frac{k_0\, v_0^2}{\nu^2} \tag{22}$$

Equations (16) to (19) are transformed to their corresponding non-dimensional form as:

$$\frac{\partial u}{\partial t} - 4\,\frac{\partial u}{\partial \eta} = 4\frac{\partial^2 u}{\partial \eta^2} - k\frac{\partial^3 u}{\partial \eta^2\, \partial t} - \frac{M}{1+m^2}\,(mw+u) + Gr\theta + GcC \tag{23}$$

$$\frac{\partial w}{\partial t} - 4\,\frac{\partial w}{\partial \eta} = 4\,\frac{\partial^2 w}{\partial \eta^2} - k\frac{\partial^3 w}{\partial \eta^2 \partial t} + \frac{M}{1+m^2}\,(mu - w) \tag{24}$$

$$\frac{\partial \theta}{\partial t} - 4\,\frac{\partial \theta}{\partial \eta} = \frac{4}{Pr}\,\frac{\partial^2 \theta}{\partial \eta^2} - F\theta \tag{25}$$

$$\frac{\partial C}{\partial t} - 4\,\frac{\partial C}{\partial \eta} = \frac{4}{Sc}\,\frac{\partial^2 C}{\partial \eta^2} \tag{26}$$

The modified boundary conditions become

$$\left.\begin{array}{l} t \le 0:\ u(\eta,t) = w(\eta,t) = \theta\,(\eta,t) = C(\eta,t) = 0 \ \text{ for all } \ \eta \\ t > 0: u(0,t) = w(0,t) = 0, \theta(0,t) = e^{i\Omega t},\ \ C(0,t) = e^{i\Omega t} \\ \qquad u(\infty,t) = w(\infty,t) = \theta\,(\infty,t) = C(\infty,t) \to 0 \end{array}\right\} \tag{27}$$

The equations (23) and (24) can be combined into a single equation by introducing the complex velocity

$$\psi \;=\; u + iw \quad \text{where} \quad i = \sqrt{-1} \tag{28}$$

giving,

$$\frac{\partial^2\psi}{\partial\eta^2} - \frac{k}{4}\,\frac{\partial^3\psi}{\partial\eta^2\,\partial t} - \frac{1}{4}\,\frac{\partial\psi}{\partial t} + \frac{\partial\psi}{\partial\eta} - \frac{M(1-im)\psi}{4(1+m^2)} \;=\; -\,\frac{Gr\theta}{4} - \frac{GcC}{4} \tag{29}$$

Again, on using equation (28), the boundary conditions in equation (27) are transformed to:

$$\left.\begin{aligned} &t \le 0 : \psi(\eta,t) = \theta\,(\eta,t) = C(\eta,t) = 0 \quad \text{for all} \quad \eta \\ &t > 0 : \psi(0,t) = 0, \theta(0,t) = C(0,t) = e^{i\Omega t} \\ &\qquad \psi(\infty,t) = \theta\,(\infty,t) = C(\infty,t) \to 0 \end{aligned}\right\} \tag{30}$$

Substituting $\theta\,(\eta,t) = e^{i\Omega t}\, f(\eta)$ in equation (25), we get

$$f''(\eta) + Prf'(\eta) - \frac{1}{4}\,(FPr + i\Omega\,Pr)f(\eta) = 0 \tag{31}$$

which has to be solved under the boundary conditions

$$f(0) = 1, f(\infty) \;=\; 0 \tag{32}$$

Hence $f(\eta) \;=\; e^{-\,\frac{\eta}{2}\left[Pr+\sqrt{Pr^2+FPr+i\Omega\,Pr}\right]}$

$$\Rightarrow\; \theta\,(\eta,t) = e^{i\Omega t-\,\frac{\eta}{2}\left[Pr+\sqrt{Pr^2+FPr+i\Omega Pr}\right]}$$

Separating real and imaginary parts, the real part is given by

$$\theta_r(\eta,t) = \left\{cos\left(\Omega t - \;\frac{\eta}{2}\,D_1 sin\frac{\alpha}{2}\right)\right\}\; e^{-\,\frac{\eta}{2}\left[Pr+D_1\,cos\frac{\alpha}{2}\right]} \tag{33}$$

Where

$$D_1 \;=\; [(Pr+F)^2 +\, \Omega^2]^{1/4}\,Pr^{1/2}\,,\, \alpha \;=\; tan^{-1}\left(\frac{\Omega}{Pr+F}\right) \tag{34}$$

Now, putting $C(\eta,t) = e^{i\Omega t}g(\eta)$ in equation (26), we get

$$g''(\eta) + Scg'(\eta) - \frac{i\Omega\, Sc}{4} g(\eta) = 0 \tag{35}$$

which has to be solved under the boundary condition

$$g(0) = 1, \quad g(\infty) \ = \ 0 \tag{36}$$

Hence, $g(\eta) \ = \ e^{-\frac{\eta}{2}\left[Sc^2+\sqrt{Sc^2+i\Omega\, Sc}\right]}$

$$\Rightarrow \ C(\eta, t) = e^{i\Omega t - \frac{\eta}{2}\left[Sc^2+\sqrt{Sc^2+i\Omega\, Sc}\right]}$$

Separating real and imaginary parts, the real part is given by

$$C_r(\eta, t) = \left\{cos\left(\Omega t - \frac{\eta}{2}\, D_2 sin\frac{\beta}{2}\right)\right\} \ e^{-\frac{\eta}{2}\left[Sc + D_2 cos\frac{\beta}{2}\right]} \tag{37}$$

where,

$$D_2 = \ [Sc^2 + \Omega^2]^{1/4} \ Sc^{1/2} \ , \ \ \beta \ = \ tan^{-1}\left(\frac{\Omega}{Sc}\right) \tag{38}$$

In order to solve equation (29), we substitute $\psi \ = \ e^{i\Omega t}F(\eta)$ and the corresponding boundary conditions now become:

$$F(0) = 0, \quad F(\infty) = 0 \tag{39}$$

On separating real and imaginary parts, we get

$$\begin{aligned} u = {} & [B_{15} cos(\Omega t - \ B_6\eta) \ - \ B_{16} sin(\Omega t - \ B_6\eta)]\, e^{-B_5\eta} \\ & - [GrB_{11} cos(\Omega t - B_2\eta) \ - \ GrB_{12}\, sin(\Omega t - \ B_2\eta)] \ e^{-B_1\eta} \\ & - [GcB_{13}\, cos(\Omega t - \ B_4\eta) - \ GcB_{14} sin(\Omega t - B_4\eta)]\, e^{-B_3\eta} \end{aligned} \tag{40}$$

$$\begin{aligned} w = {} & [B_{16} cos(\Omega t - \ B_6\eta) \ + \ B_{15} sin(\Omega t - B_6\eta)]\, e^{-B_5\eta} \\ & - [GrB_{12} cos(\Omega t - \ B_2\eta) \ + \ GrB_{11} sin(\Omega t - \ B_2\eta)]\, e^{-B_1\eta} \\ & - [GcB_{14} cos(\Omega t - B_4\eta) \ + \ GcB_{13} sin(\Omega t - \ B_4\eta)]\, e^{-B_3\eta} \end{aligned} \tag{41}$$

If τ_1 and τ_2 are the axial and the transverse components of skin-friction respectively, then

$$\tau_1 + \; i\tau_2 \; = \; \mu \; \left(\frac{\partial \psi}{\partial \eta}\right)_{\eta=0}$$

In non-dimensional form τ_1 becomes

$$\tau_1 = \; \left(\frac{\partial u}{\partial \eta}\right)_{\eta=0} \; = \; B_5B_{16} + B_6B_{15} - \; Gr(B_1B_{12} + B_2B_{11}) - \quad (42)$$

$$Gc(B_3B_{14} + B_4B_{13})$$

Similarly, shearing stress at the wall along z-axis is given by

$$\tau_2 = \; \left(\frac{\partial w}{\partial \eta}\right)_{\eta=0} \; = \; - B_5B_{15} + B_6B_{16} + Gr(B_1B_{11} - B_2B_{12}) + \quad (43)$$

$$Gc(B_3B_{13} - B_4B_{14})$$

From the temperature field, the heat transfer coefficient in terms of Nusselt number is given by:

$$Nu = - \; \frac{\partial \theta_r(\eta, t)}{\partial \eta} \; \Big|_{\eta=0}$$

$$= \; \frac{1}{2} \; \left[Pr cos \Omega t + D_1 cos \left(\Omega t + \frac{\alpha}{2}\right)\right] \quad (44)$$

Further from the concentration field, the coefficient of mass transfer in terms of Sherwood number is given by

$$Sh = - \; \frac{\partial C_r(\eta, t)}{\partial \eta} \; \Big|_{\eta=0}$$

$$= \; \frac{1}{2} \; \left[Sc cos \Omega t + D_2 cos \left(\Omega t + \frac{\beta}{2}\right)\right] \quad (45)$$

where,

$$B_1 = \; \frac{1}{2} \; \left[Pr + D_1 cos \frac{\alpha}{2}\right] \quad , \qquad B_2 = \; \frac{D_1}{2} \, sin \frac{\alpha}{2},$$

$$B_3 \;=\; \frac{1}{2}\left[Sc + D_2\, cos\frac{\beta}{2}\right]\;, \quad B_4 = \;\frac{D_2}{2}\, sin\frac{\beta}{2},$$

$$D_3 \;=\; \left[\left[1 + \;\frac{M}{1+m^2} \;-\; \frac{k\,\Omega}{4}\,\left(\frac{Mm}{1+m^2}\;-\;\Omega\right)\right]^2 + \;\left[\Omega \;-\; \frac{4Mm + k\,\Omega\, M}{4(1+m^2)}\right]^2\right]^{1/4}$$

$$\gamma = tan^{-1}\,\left[\frac{\Omega\;-\;\left(\frac{4Mm+k\Omega M}{4(1+m^2)}\right)}{1+\;\frac{M}{1+m^2}\;-\;\frac{k\,\Omega}{4}\,\left(\frac{Mm}{1+m^2}\;-\;\Omega\right)}\right], \quad D_4 \;=\; k\Omega/4$$

$$B_5 \;=\; \frac{1+\;D_3\;\left(cos\frac{\gamma}{2}\;-\;D_4 sin\frac{\gamma}{2}\right)}{2(1+\;D_4^2)}, \quad B_6 = \;\frac{D_4 + \;D_3\;\left(D_4 cos\frac{\gamma}{2}\;+\;sin\frac{\gamma}{2}\right)}{2(1+D_4^2)}$$

$$B_7 = \;4(B_1^2 -\;B_2^2)\;+\;2B_1\,B_2\,k\Omega\;+\;4B_1 -\;M/1+m^2$$

$$B_8 \;=(B_1^2 -\;B_2^2)k\Omega\;-\;8B_1B_2 -\;4B_2 +\;\Omega\;-\;Mm/1+m^2$$

$$B_9 \;=\;4(B_3^2 -\;B_4^2)\;+\;2k\Omega\,B_3B_4 +\;4B_3\;-\;\frac{M}{1+m^2}$$

$$B_{10} = \;-\,8B_3\,B_4 + \;k\Omega\,(B_3^2 -\;B_4^2)\;-\;4B_4 + \Omega\;-\;\frac{Mm}{1+m^2}$$

$$B_{11} \;=\;\frac{B_7}{B_7^2\;+\;B_8^2}\;,\;\; B_{12}\;=\;\frac{B_8}{B_7^2\;+\;B_8^2}\;,$$

$$B_{13} \;=\;\frac{B_9}{B_9^2\;+\;B_{10}^2}\;,\;\; B_{14}\;=\;\frac{B_{10}}{B_9^2 +\;B_{10}^2}$$

$$B_{15} = \;GrB_{11} +\;GcB_{13}\;,\quad B_{16}\;=\;GrB_{12} +\;GcB_{14}.$$

3 Discussion and conclusion

In order to illustrate the influence of various parameters on the velocity, temperature, concentration fields, shearing stress, rate of heat and mass transfer, numerical calculations of the solutions, obtained in the preceding section, have been carried out for both cases corresponding to cooling and heating of the porous plate by free convection currents. The value of Prandtl number is taken equal to 3 which physically correspond to Freon. Freon represents several different chlorofluorocarbons or CFC_s which are used in commerce and industry.

Figures 1 and 2 depict the primary velocity profiles u against η for cooling ($Gr > 0$) and heating ($Gr < 0$) of the plate by free-convection currents taking different values of Ω (frequency), F (radiation parameter), Sc (Schmidt number), M (Magnetic parameter), k (visco-elastic parameter) and m (Hall parameter). From figure 1 it is seen that for higher values of frequency the velocity is of oscillatory nature ; however as Ω decreases the oscillations in the profiles get damped. The velocity is greater for Ammonia ($Sc = 0.78$, at 25^0C temperature and 1 atmospheric pressure) than for Helium ($Sc = 0.30$, at 25^0C temperature and 1 atmospheric pressure). The effect of increasing magnetic parameter is to enhance the primary velocity but on moving farther away from the plate ($\eta > 6$) this behaviour reverses. This figure further indicates that primary velocity decreases with increase in Hall parameter. Moreover, the velocity of Newtonian fluid ($k = 0$) is more than the velocity of non-Newtonian fluid ($k \neq 0$). On increasing the radiation parameter (F), the values of u differed only by small amounts therefore the curves could not be shown distinctly in the figures. From figure 2 it is revealed that the involved parameters exhibit similar behaviour for heating of the plate ($Gr < 0$) like in case of cooling of the plate.

The secondary velocity profiles w for cooling of the plate are plotted in figure 3 and the profiles due to heating of the porous plate are depicted in figure 4. The analysis of the graphs reveals that on increasing the values of frequency (Ω) parameter, a sharp rise in the magnitude of velocity profiles is observed near the plate but at a certain distance away from the plate it falls rapidly and finally decay to the free stream value. A close examination of the data presented in figure 3 shows that the radiation parameter tends to reduce the fluid velocity in secondary flows for $Gr >$

0 but reverse happens for the case $Gr < 0$. The retardation in the secondary velocity field due to the increase in magnetic parameter and Hall parameter is noticed for $Gr > 0$ and $Gr < 0$. This observation can be explained by the fact that as M increases, the Lorentz force, which opposes the flow, also increases and leads to enhanced deceleration of the flow. The velocity of Helium is greater than the velocity of Ammonia in secondary flows. Further, it is seen from these figures that w-component of velocity of Newtonian fluid is lower than that of visco-elastic fluid. For both the cases under consideration ($Gr > 0$ and $Gr < 0$) it turns out that the maximum velocity occurs in the vicinity of the plate and as $\eta \to \infty$ the velocity profiles terminate to zero.

Figure 5 represents the temperature profiles θ_r against η for different values of Pr, Ω and F taking $\Omega t = \pi/2$. In the neighborhood of the surface the temperature profiles become maximum and then decreases and finally take asymptotic values.

The thermal boundary layer thickness is greater for fluids with small Prandtl number. The reason is that smaller values of Pr are equivalent to increasing thermal conductivity and therefore heat is able to diffuse away from the heated surface more rapidly than for higher values of Pr. It is observed that the temperature rises with increasing frequency. Moreover, the effect of radiation is to increase the rate of energy transport to the fluid and accordingly increase the fluid temperature.

Figure 6 displays concentration profiles Cr vs. η for various gases like Hydrogen ($Sc = 0.22$), Helium ($Sc = 0.30$), Watervapour ($Sc = 0.60$), Oxygen ($Sc = 0.66$) and Ammonia ($Sc = 0.78$) taking $\Omega t = \pi/2$. It is reported that the effect of increasing values of Schimdt number (Sc) is to decrease the concentration profiles. This is consistent with the fact that the increase of Sc means a decrease of molecular diffusivity (D) that result in decrease of concentration boundary layer. Hence the concentration of species is higher for smaller value of Sc and lower for larger value of Sc. Furthermore, it is observed that near the boundary the thickness of concentration boundary layer increases significantly with increasing frequency but opposite trend is noted far away from the plate ($\eta > 4$).

Figures 7 and 8 illustrate the effects of F, Sc, M and k on shearing stress along x-axis τ_1 for cooling and heating of the plate respectively while the shearing stress along z-axis τ_2 is shown in figure 9. The axial and the transverse components of skin-friction are plotted against Hall parameter. It is observed that for $Sc = 0.30$ both τ_1 and τ_2 decreases with increasing m for $Gr > 0$ and $Gr < 0$ but for $Sc = 0.78$ the shearing stress along x-axis and z-axis increases with increasing m. Further, since the velocity in primary flows increases with increasing M therefore τ_1 also increases as M increases, because the friction increases as the fluid velocity increases. Similarly, the velocity in secondary flows decreases as M increases therefore τ_2 also exhibit similar behaviour for increasing M. Due to an increase in F, the velocity gradient in primary flows increases, but the velocity gradient in secondary flows decreases for $Gr > 0$ while reverse happens for the case $Gr < 0$. Finally, it is seen that the transverse component of skin-friction τ_2 is lower for non-Newtonian fluid as compared to Newtonian fluid but opposite trend is noted for the axial component of skin friction τ_1. Figures 8 and 9 reveal that since the Hall parameter (m) gives rise to the secondary flow field, the transverse component of skin friction is greater than the axial component of skin friction at and near the wall.

The quantity of heat exchanged between the body and the fluid is given by temperature gradient Nu (Nusselt Number) which is given below in Table I.

Table 1: Rate of heat transfer (Nu)

	Nu		
Ω	**F**	**Pr = 3.0**	**Pr = 5.0**
1.0	1.0	- 0.786	- 1.169
2.0	1.0	- 0.902	- 1.286
3.0	1.0	- 1.018	- 1.404
1.0	2.0	- 1.145	- 1.673

It is inferred that the rate of heat transfer Nu falls with increasing values of Prandtl number. Further it is noticed that higher values of frequency and radiation parameter reduces temperature gradient. Rate of mass transfer Sh (Sherwood number) for different values of Sc and Ω is shown below in table II.

It is revealed that Sh is greater for lower values of Sc and Ω.

Table 2: Rate of mass transfer (Sh)

	Sh		
Ω	**Sc = 0. 22**	**Sc = 0.30**	**Sc = 0.78**
1.0	- 0. 105	- 0. 124	- 0. 251
2.0	- 0.180	- 0.214	- 0.372
3.0	- 0.241	- 0. 283	- 0.474
4.0	- 0.291	- 0. 341	- 0.562

References

[1] Baehr, H.D. and Stephan, K. (1998): Heat and mass transfer. Springer-Verlag, Berlin.

[2] Soundalgekar, V.M. (1977): Free convection effects on the Stokes problem for an infinite vertical plate. Transactions of the ASME Journal of Heat Transfer, Vol. 99, pp.499-501.

[3] Soundalgekar, V.M. and Wavre, P.D. (1977): Unsteady free convection flow past an infinite vertical plate with constant suction and mass transfer. Int. J. Heat Mass Transfer, Vol.20, pp.1363-1373.

[4] Perdikis, C. (1986): Free convection and mass transfer effects on the flow past a vertical plate. Astrophysics and Space Science, Vol. 119, pp.295-303.

[5] Lin, H.T. and Wu, C.M. (1995): Combined heat and mass transfer by laminar natural convection from a vertical plate. Heat and Mass Transfer, Vol.30, pp.369-376.

[6] Georgantopoulos, G.A.; Koullias, J.; Goudas, C.L. and Courogenis, C. (1981): Free convection and mass transfer effects on the hydromagnetic oscillatory flow past an infinite vertical porous plate. Astrophysics and Space Science, Vol.74, pp.357-389.

[7] Helmy, K.A. (1999): MHD unsteady free convection flow past a vertical porous plate. ZAMM, Vol.78, pp.225-270.

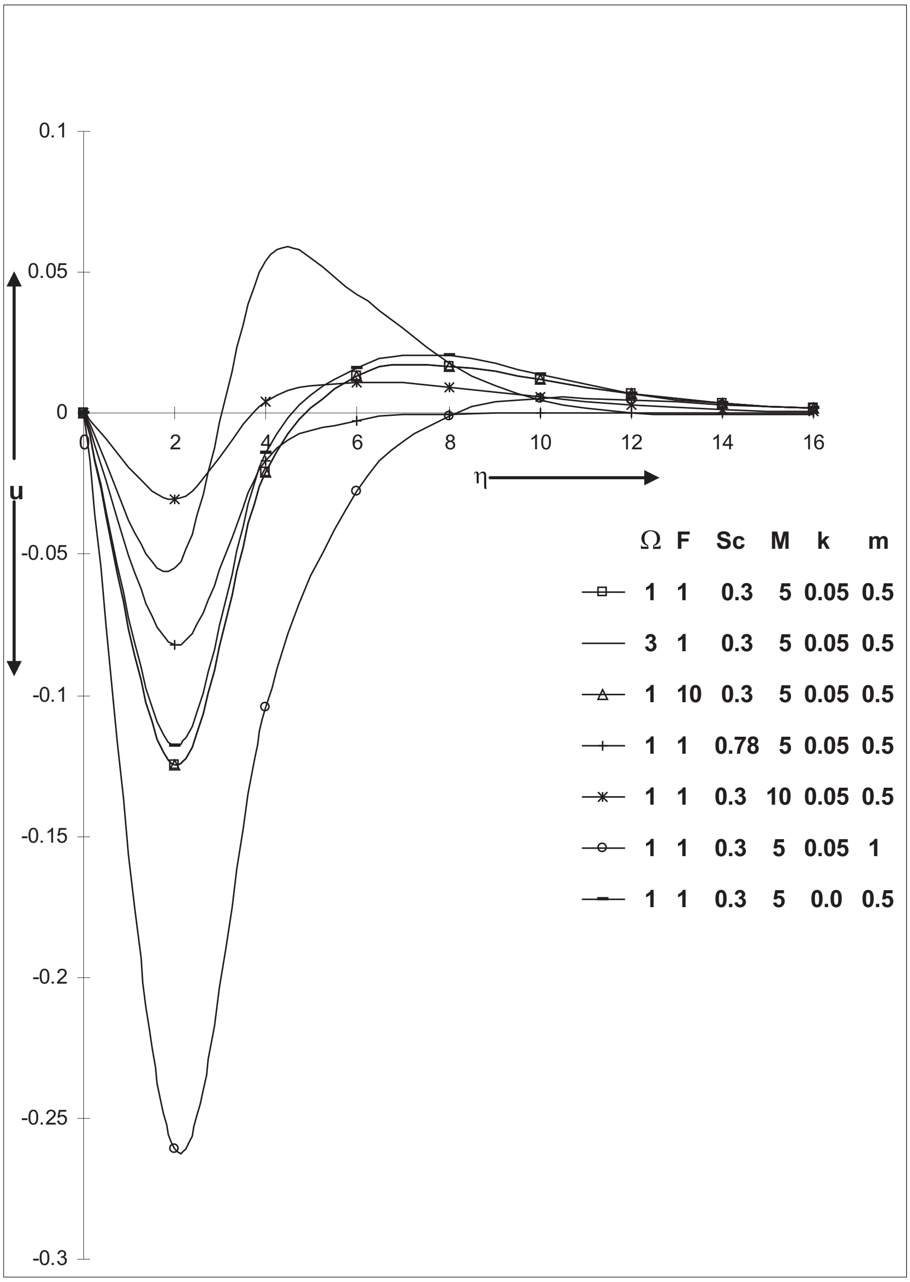

Figure 1: Variation of velocity component u for $Pr = 3.0$, $Gc = 2.0$, $Gr = 5.0$; $\Omega t = \pi/2$.

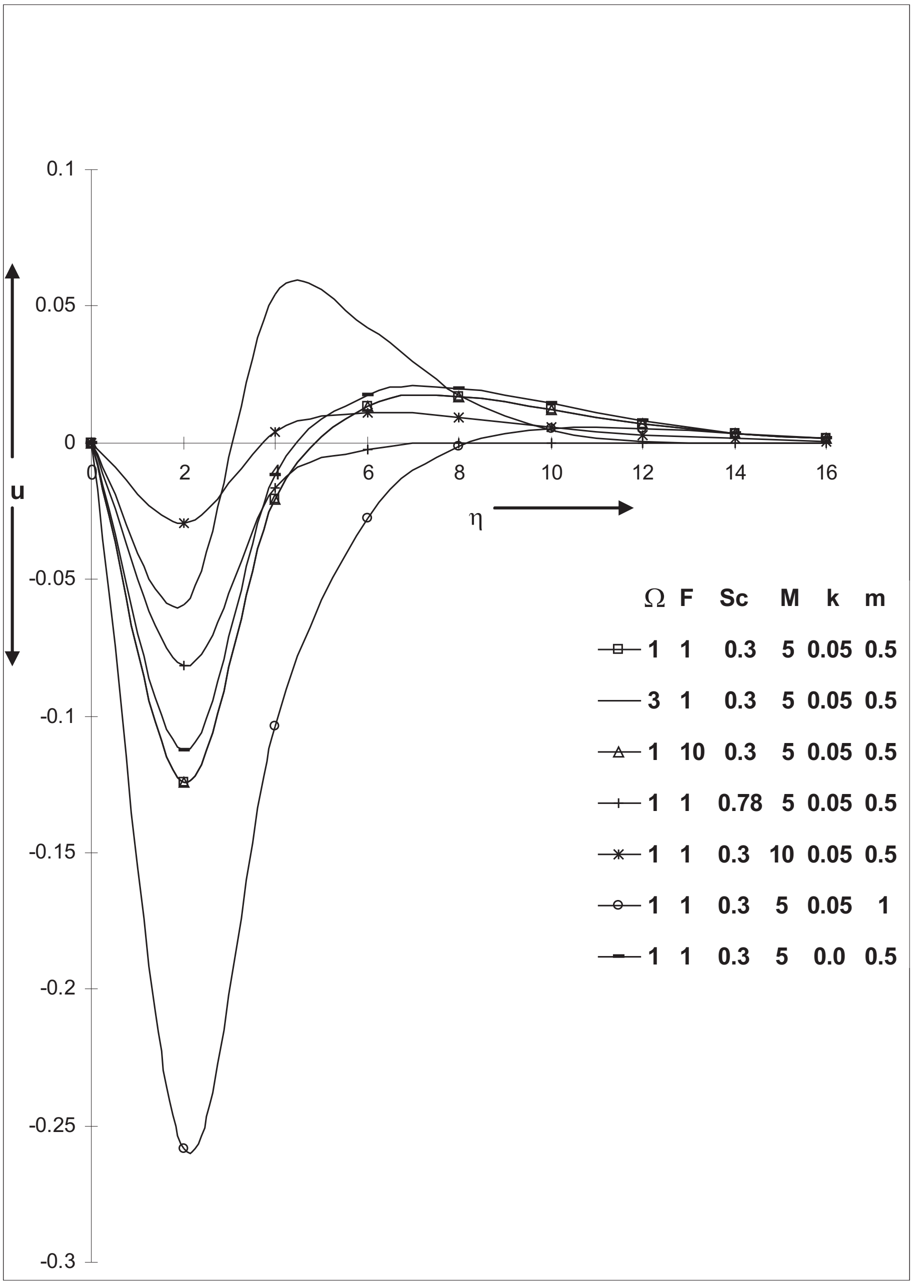

Figure 2: Variation of velocity component u for $Pr = 3.0$, $Gc = 2.0$, $Gr = -5.0$; $\Omega t = \pi/2$.

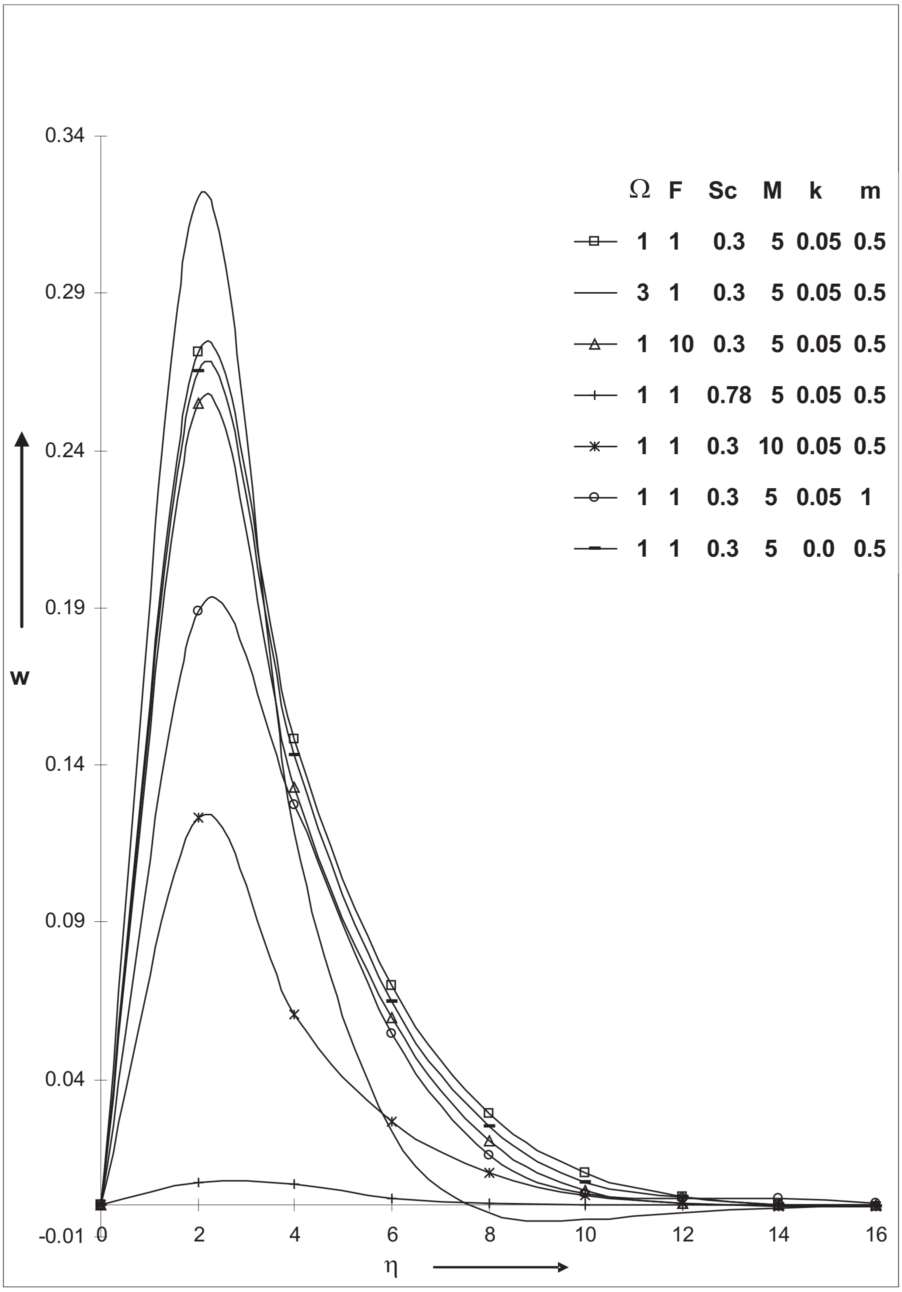

Figure 3: Variation of velocity component w for $Pr = 3.0$, $Gc = 2.0$, $Gr = 5.0$; $\Omega t = \pi/2$.

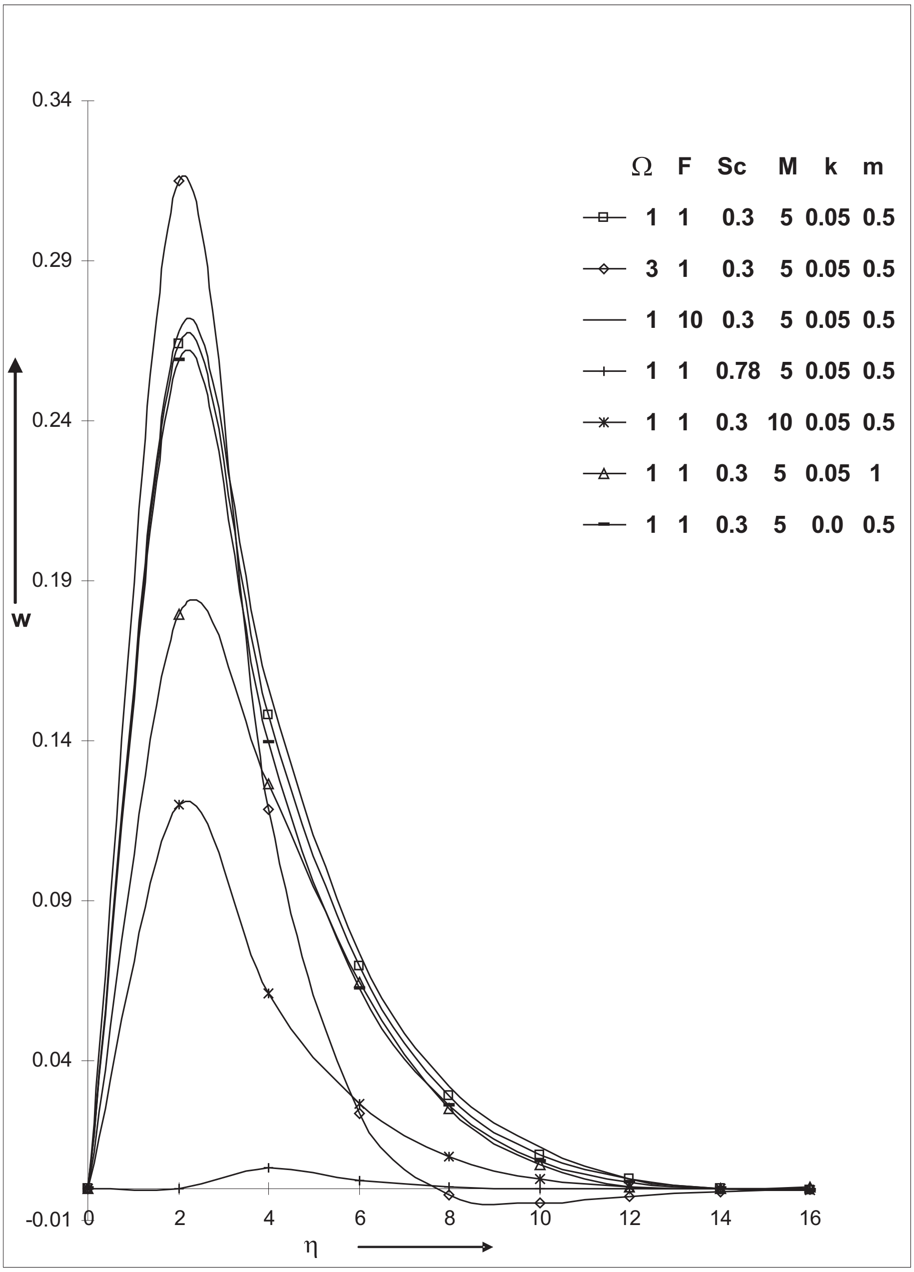

Figure 4: Variation of velocity component w for $Pr = 3.0,\ Gc = 2.0,\ Gr = -5.0;\ \Omega t = \pi/2$.

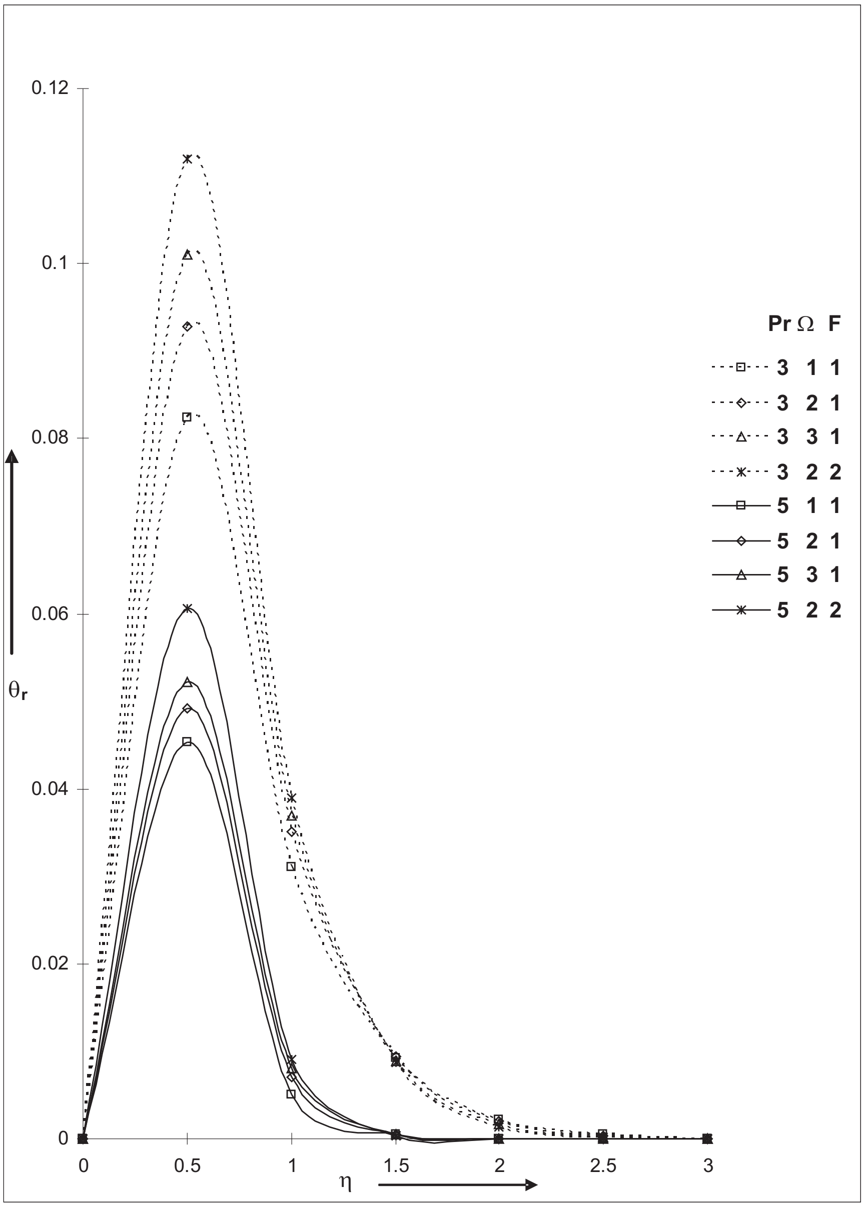

Figure 5: Variation of temperature Θ_r.

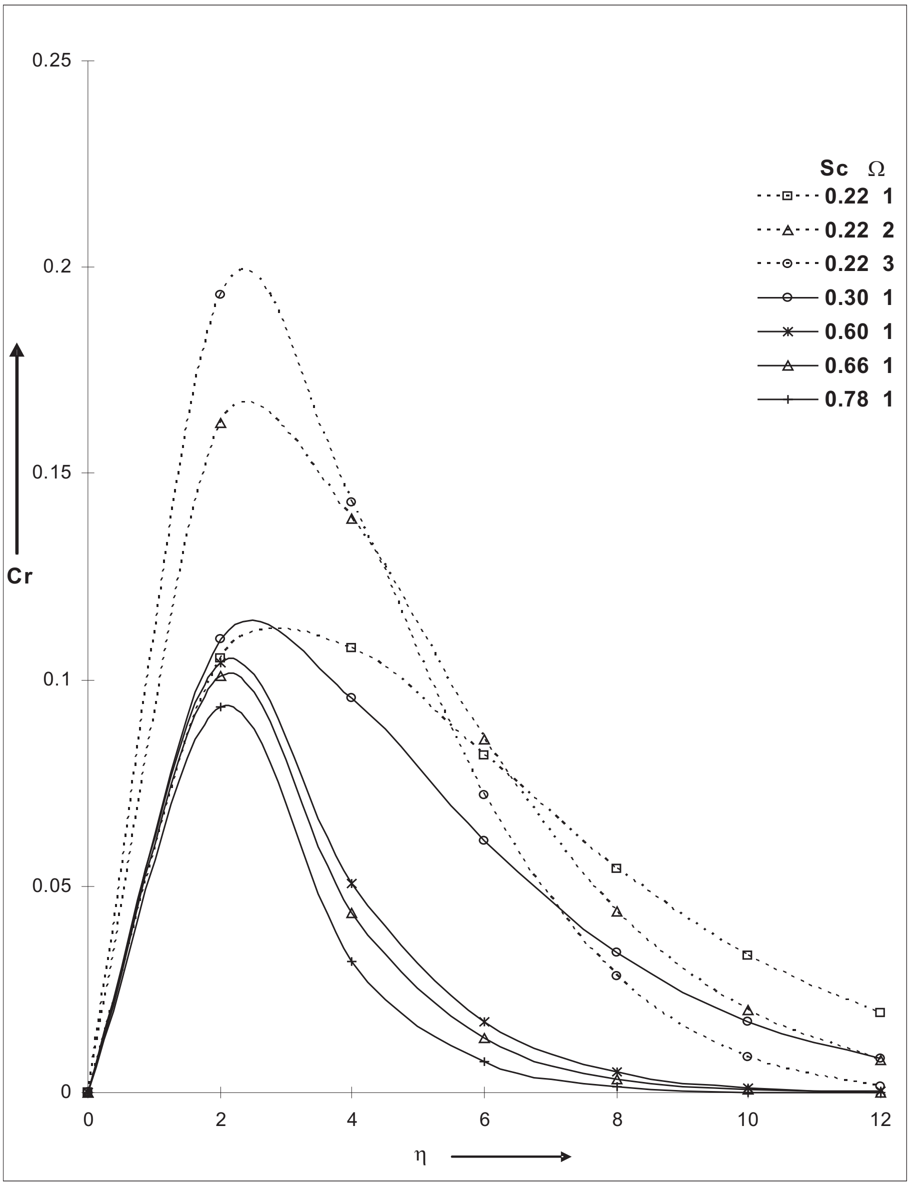

Figure 6: Variation of concentration C_r

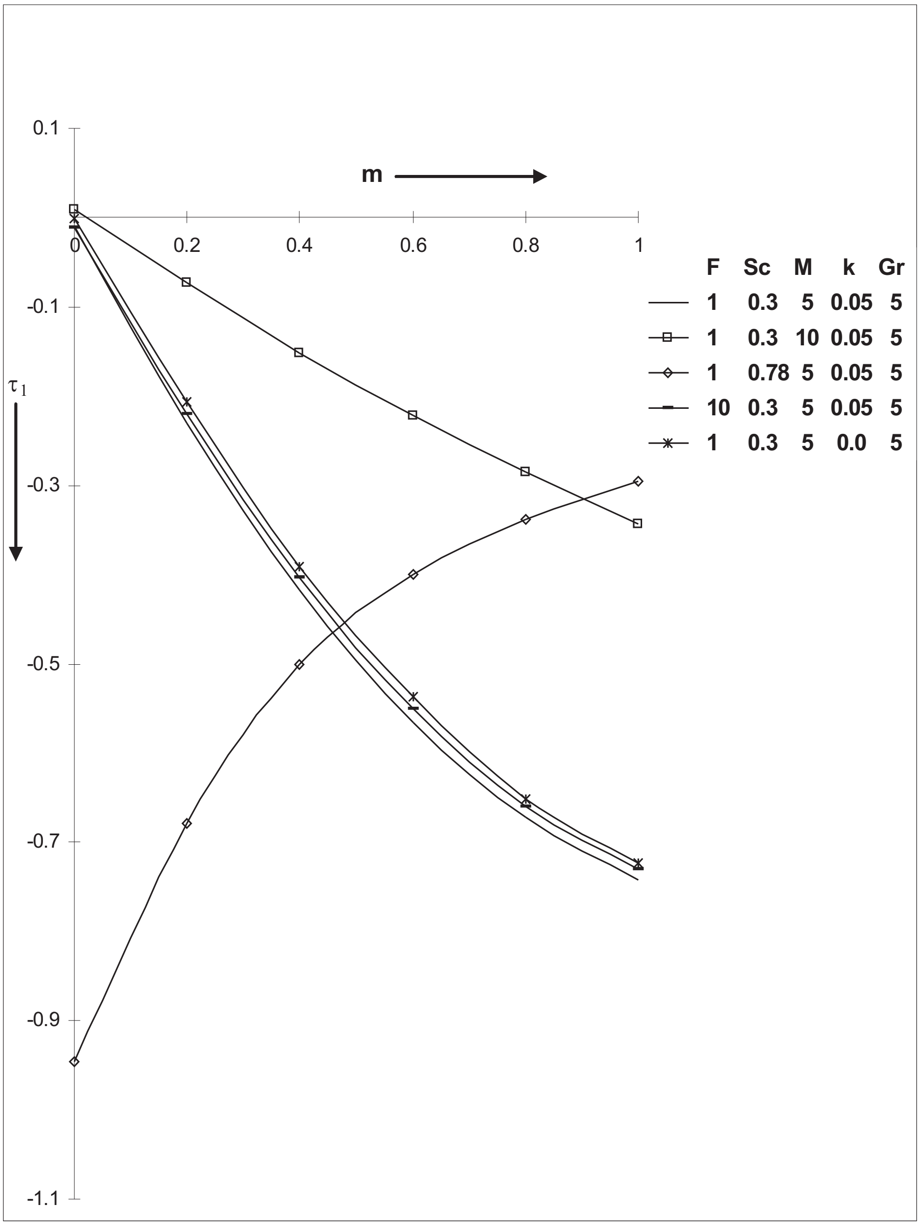

Figure 7: Variation of shearing stress τ_1 for $Pr = 3.0,\ Gc = 2.0,\ \Omega = 1.0,\ \Omega t = \pi/2$.

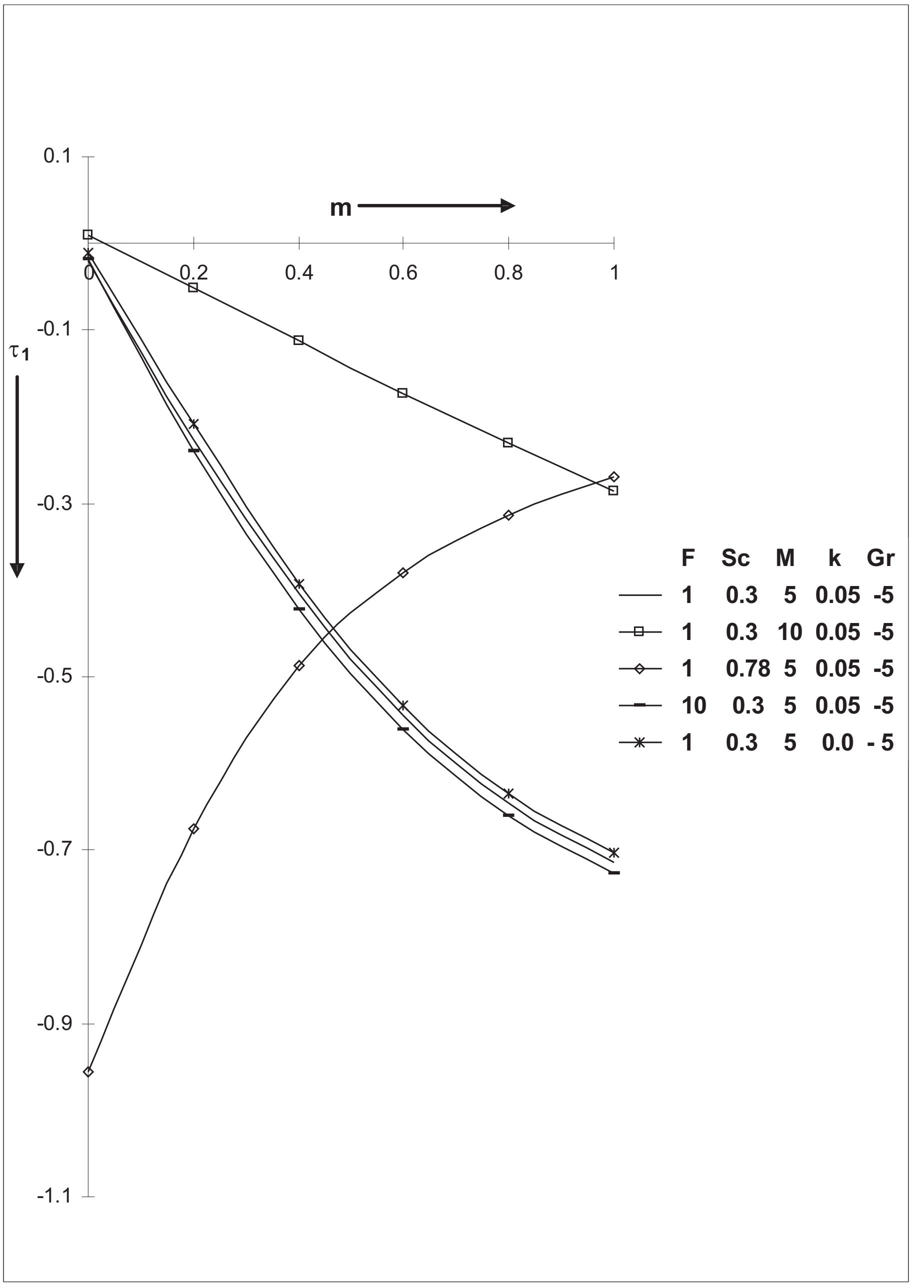

Figure 8: Variation of shearing stress τ_1 for $Pr = 3.0,\ Gc = 2.0,\ \Omega = 1.0,\ \Omega t = \pi/2$.

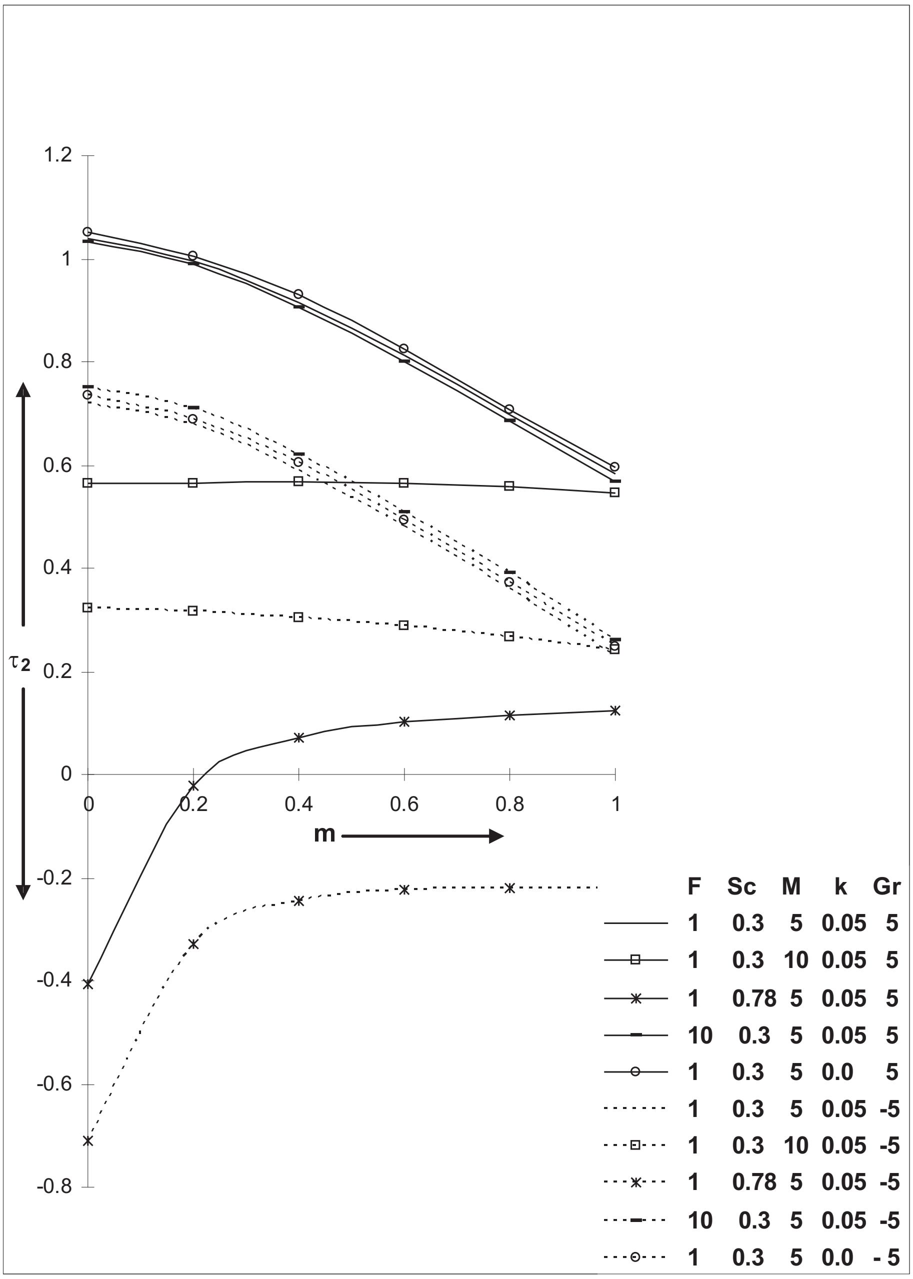

Figure 9: Variation of shearing stress τ_2 for $Pr = 3.0,\ Gc = 2.0,\ \Omega = 1.0,\ \Omega t = \pi/2$.

[8] Katagiri, M. (1969): The effect of Hall current in the MHD boundary layer flow past a semi-infinite plate. J. Phys. Soc. Japan, Vol.27, pp.1051-1059.

[9] Hossain, M.A. (1986): Effect of Hall current on unsteady hydromagnetic free convection flow near an infinite vertical porous plate. J. Phys. Soc. Japan, Vol.55, pp.2183-2190.

[10] Hossain, M.A. and Mohammad, K. (1988): Effect of Hall current on hydromagnetic free convection flow near an accelerated porous plate. Jpn. J. Appl. Phys., Vol.27, pp.1531-1535.

[11] Pop, I. and Watanabe, T. (1994): Hall effects on magnetohydrodynamic free convection about a semi-infinite vertical flat plate. Int. J. Engg. Sci., Vol.32, pp.1903-1911.

[12] Acharya, M.; Dash, G.C. and Singh, L.P. (1995): Effect of chemical and thermal diffusion with Hall current on unsteady hydromagnetic flow near an infinite vertical porous plate. J. Phys. D: Appl. Phys., Vol.28, pp.2455-2464.

[13] Hossain, M.A. and Rashid, R.I.M.A. (1987): Hall effect on hydromagnetic free convection flow along a porous flat plate with mass transfer. J. Phys. Soc. Japan, Vol.56, pp.97-104.

[14] Aboeldahab, E.M. and Elbarbary, E.M.E. (2001): Hall current effect magnetohydrodynamics free convection flow past a semi-infinite vertical plate with mass transfer. Int. J. Engg. Sci., Vol.39, pp.1641-1652.

[15] Takhar, H.S.; Roy, S. and Nath, G. (2003): Unsteady free convection flow over an infinite vertical porous plate due to the combined effects of thermal and mass diffusion, magnetic field and Hall currents. Heat and Mass Transfer, Vol.39, pp.825-834.

[16] Soundalgekar, V.M. and Takhar, H.S. (1993): Radiative free convection flow of a gas past a semi-infinite vertical plate. Modelling, Measurement & Control, Vol. B51, pp.31-40.

[17] Takhar, H.S.; Gorla, R.S.R. and Soundalgekar, V.M. (1996): Radiation effects on MHD free convection flow of a gas past a semi-infinite vertical plate. International Journal of Numerical Methods for Heat & Fluid Flow, Vol.6, pp.77-83.

[18] Hossain, M.A. and Takhar, H.S. (1996): Radiation effect on mixed convection along a vertical plate with uniform surface temperature. Heat and Mass Transfer, Vol.31, pp.243-248.

[19] Abo-eldahab, E.M. (2004): The effects of temperature-dependent fluid properties on free convective flow along a semi-infinite vertical plate by the presence of radiation. Heat and Mass Transfer, Vol.41, pp.163-169.

[20] Muthucumaraswamy, R. and Kumar, G.S. (2004): Heat and mass transfer effects on moving vertical plate in the presence of thermal radiation. Theoret. Appl. Mech., Vol.31, pp.35-46.

[21] Kinyanjui, M.; Kwanza, J.K. and Uppal, S.M. (2001): Magnetohydrodynamic free convection heat and mass transfer of a heat generating fluid past an impulsively started infinite vertical porous plate with Hall current and radiation absorption. Energy Conservation and Management, Vol.42, pp.917-931.

[22] Rajagopal, K.R. (1983): On Stokes problem for a non-Newtonian fluid. Acta Mechanica, Vol.48, pp.233-239.

[23] Chowdhury, M.K. and Islam, M.N. (2000): MHD free convection flow of visco-elastic fluid past an infinite vertical porous plate. Heat and Mass Transfer, Vol.36, pp.439-447.

[24] Bestman, A.R. (1985): Free convection heat transfer to steady radiating non-Newtonian MHD flow past a vertical porous plate. International Journal for Numerical Methods in Engineering, Vol.21, pp.899-908.

[25] Walters, K. (1964): On second – order effect in elasticity, plasticity and fluid dynamics. IUTAM Int. Symp. (Reiner, M. and Abir, D. eds.), Pergamon Press, New York.

[26] Cogley, A.C non-gray gas near equilibrium. AIAAJ.; Vincenti, W.G. and Giles, S.E. (1963): Differential approximation for radiative transfer in a, Vol. 6, pp.551-553.

Submitted on November 2006.

Halov efekt na MHD konvekciono strujanje viskoelastičnog fluida preko beskonačne vertikalne porozne ploče sa prenosom mase i zračenjem

UDK 539.42, 539.421

Posmatra se nestacionarno hidromagnetsko strujanje viskoelastičnog fluida sa zračeće vertikalne porozne ploče sa prenosom mase i uzimanjem u obzir Halovih struja. Rezultujući problem je rešen analitički i dobijena su eksplicitna rešenja za rasporede brzine, temperature i koncentracije kao i za smičući napon, brzinu promene toplote kao i prenos mase na zidu.

Uticaj raznih parametara kao: Halovog parametra, magnetskog parametra, viskoelastičnog parametra, frekventnog parametra itd. na tečenje je prikazan slikama i tabelama.